Ultra-high-speed wavelength conversion in a silicon photonic chip

Hu, Hao; Ji, Hua; Galili, Michael; Pu, Minhao; Peucheret, Christophe; Mulvad, Hans Christian Hansen; Yvind, Kresten; Hvam, Jørn Märcher; Jeppesen, Palle; Oxenløwe, Leif Katsuo

Published in:
Optics Express

Publication date:
2011

Document Version
Publisher's PDF, also known as Version of record

Ultra-high-speed wavelength conversion in a silicon photonic chip

Hao Hu,* Hua Ji, Michael Galili, Minhao Pu, Christophe Peucheret, Hans Christian, H. Mulvad, Kresten Yvind, Jørn M. Hvam, Palle Jeppesen, and Leif K. Oxenløwe

DTU Fotonik, Department of Photonics Engineering, Technical University of Denmark, Ørsteds Plads, Building 343, DK-2800 Kgs. Lyngby, Denmark
**huhao@fotonik.dtu.dk*

Abstract: We have successfully demonstrated all-optical wavelength conversion of a 640-Gbit/s line-rate return-to-zero differential phase-shift keying (RZ-DPSK) signal based on low-power four wave mixing (FWM) in a silicon photonic chip with a switching energy of only ~110 fJ/bit. The waveguide dispersion of the silicon nanowire is nano-engineered to optimize phase matching for FWM and the switching power used for the signal processing is low enough to reduce nonlinear absorption from two-photon-absorption (TPA). These results demonstrate that high-speed wavelength conversion is achievable in silicon chips with high data integrity and indicate that high-speed operation can be obtained at moderate power levels where nonlinear absorption due to TPA and free-carrier absorption (FCA) is not detrimental. This demonstration can potentially enable high-speed optical networks on a silicon photonic chip.

OCIS codes: (060.2330) Fiber optics communications; (230.7405) Wavelength conversion devices; (070.4340) Nonlinear optical signal processing.

References and links

1. D. J. Blumenthal, P. R. Prucnal, and J. R. Sauer, "Photonic packet switches: architectures and experimental implementations," Proc. IEEE **82**(11), 1650–1667 (1994).
2. D. Cotter, R. J. Manning, K. J. Blow, A. D. Ellis, A. E. Kelly, D. Nesset, I. D. Phillips, A. J. Poustie, and D. C. Rogers, "Nonlinear Optics for High-Speed Digital Information Processing," Science **286**(5444), 1523–1528 (1999).
3. K. Hinton, G. Raskutti, P. M. Farrell, and R. S. Tucker, "Switching energy and device size limits on digital photonic signal processing technologies," IEEE J. Sel. Top. Quantum Electron. **14**(3), 938–945 (2008).
4. D. A. B. Miller, "Are optical transistors the logical next step?" Nat. Photonics **4**(1), 3–5 (2010).
5. V. R. Almeida, C. A. Barrios, R. R. Panepucci, and M. Lipson, "All-optical control of light on a silicon chip," Nature **431**(7012), 1081–1084 (2004).
6. J. I. Dadap, N. C. Panoiu, X. Chen, I.-W. Hsieh, X. Liu, C.-Y. Chou, E. Dulkeith, S. J. McNab, F. Xia, W. M. J. Green, L. Sekaric, Y. A. Vlasov, and R. M. Osgood, Jr., "Nonlinear-optical phase modification in dispersion-engineered Si photonic wires," Opt. Express **16**(2), 1280–1299 (2008).
7. X. Liu, R. M. Osgood, Y. A. Vlasov, and W. M. J. Green, "Mid-infrared optical parametric amplifier using silicon nanophotonic waveguides," Nat. Photonics **4**(8), 557–560 (2010).
8. H. Fukuda, K. Yamada, T. Shoji, M. Takahashi, T. Tsuchizawa, T. Watanabe, J. Takahashi, and S. Itabashi, "Four-wave mixing in silicon wire waveguides," Opt. Express **13**(12), 4629–4637 (2005).
9. M. A. Foster, A. C. Turner, J. E. Sharping, B. S. Schmidt, M. Lipson, and A. L. Gaeta, "Broad-band optical parametric gain on a silicon photonic chip," Nature **441**(7096), 960–963 (2006).
10. R. Salem, M. A. Foster, A. C. Turner, D. F. Geraghty, M. Lipson, and A. L. Gaeta, "Signal regeneration using low-power four-wave mixing on silicon chip," Nat. Photonics **2**(1), 35–38 (2008).
11. F. Li, M. Pelusi, D.-X. Xu, A. Densmore, R. Ma, S. Janz, and D. J. Moss, "Error-free all-optical demultiplexing at 160Gb/s via FWM in a silicon nanowire," Opt. Express **18**(4), 3905–3910 (2010).
12. H. Ji, H. Hu, M. Galili, L. K. Oxenlowe, M. Pu, K. Yvind, J. M. Hvam, and P. Jeppesen, "Optical waveform sampling and error-free demultiplexing of 1.28 Tbit/s serial data in a silicon nanowire," in *National Fiber Optic Engineers Conference*, OSA Technical Digest (CD) (Optical Society of America, 2010), paper PDPC7.
13. C. Koos, P. Vorreau, T. Vallaitis, P. Dumon, W. Bogaerts, R. Baets, B. Esembeson, I. Biaggio, T. Michinobu, F. Diederich, W. Freude, and J. Leuthold, "All-optical high-speed signal processing with silicon-organic hybrid slot waveguidesx," Nat. Photonics **3**(4), 216–219 (2009).
14. R. Espinola, J. Dadap, R. Osgood, Jr., S. McNab, and Y. Vlasov, "C-band wavelength conversion in silicon photonic wire waveguides," Opt. Express **13**(11), 4341–4349 (2005).

#152339 - $15.00 USD Received 3 Aug 2011; revised 30 Aug 2011; accepted 30 Aug 2011; published 26 Sep 2011

15. Q. Lin, J. Zhang, P. M. Fauchet, and G. P. Agrawal, "Ultrabroadband parametric generation and wavelength conversion in silicon waveguides," Opt. Express **14**(11), 4786–4799 (2006).
16. M. A. Foster, A. C. Turner, R. Salem, M. Lipson, and A. L. Gaeta, "Broad-band continuous-wave parametric wavelength conversion in silicon nanowaveguides," Opt. Express **15**(20), 12949–12958 (2007).
17. A. C. Turner-Foster, M. A. Foster, R. Salem, A. L. Gaeta, and M. Lipson, "Frequency conversion over two-thirds of an octave in silicon nanowaveguides," Opt. Express **18**(3), 1904–1908 (2010).
18. S. Zlatanovic, J. S. Park, S. Moro, J. M. C. Boggio, I. B. Divliansky, N. Alic, S. Mookherjea, and S. Radic, "Mid-infrared wavelength conversion in silicon waveguides using ultracompact telecom-band-derived pump source," Nat. Photonics **4**(8), 561–564 (2010).
19. B. G. Lee, A. Biberman, A. C. Turner-Foster, M. A. Foster, M. Lipson, A. L. Gaeta, and K. Bergman, "Demonstration of broadband wavelength conversion at 40 Gb/s in silicon waveguides," IEEE Photon. Technol. Lett. **21**(3), 182–184 (2009).
20. Y.-H. Kuo, H. Rong, V. Sih, S. Xu, M. Paniccia, and O. Cohen, "Demonstration of wavelength conversion at 40 Gb/s data rate in silicon waveguides," Opt. Express **14**(24), 11721–11726 (2006).
21. N. Ophir, A. Biberman, A. C. Turner-Foster, M. A. Foster, M. Lipson, A. L. Gaeta, and K. Bergman, "First 80-Gb/s and 160-Gb/s wavelength-converted data stream measurements in a silicon waveguide," in *Optical Fiber Communication Conference*, OSA Technical Digest (CD) (Optical Society of America, 2010), paper OWP5.
22. H. Hu, H. Ji, M. Galili, M. Pu, H. C. Hansen Mulvad, L. Oxenløwe, K. Yvind, J. M. Hvam, and P. Jeppesen, "Silicon chip based wavelength conversion of ultra-high repetition rate data signals," in *Optical Fiber Communication Conference*, OSA Technical Digest (CD) (Optical Society of America, 2011), paper PDPA8.
23. J. Leuthold, C. Koos, and W. Freude, "Nonlinear silicon photonics," Nat. Photonics **4**(8), 535–544 (2010).
24. S. J. B. Yoo, "Wavelength conversion technologies for WDM network applications," J. Lightwave Technol. **14**(6), 955–966 (1996).
25. H. Hu, E. Palushani, M. Galili, H. C. H. Mulvad, A. Clausen, L. K. Oxenløwe, and P. Jeppesen, "640 Gbit/s and 1.28 Tbit/s polarisation insensitive all optical wavelength conversion," Opt. Express **18**(10), 9961–9966 (2010).
26. M. Galili, L. K. Oxenlowe, H. C. H. Mulvad, A. T. Clausen, and P. Jeppesen, "Optical wavelength conversion by cross-phase modulation of data signals up to 640 Gb/s," IEEE J. Sel. Top. Quantum Electron. **14**(3), 573–579 (2008).
27. Y. Liu, E. Tangdiongga, Z. Li, H. de Waardt, A. M. J. Koonen, G. D. Khoe, X. Shu, I. Bennion, and H. J. S. Dorren, "Error-free 320-Gb/s all-optical wavelength conversion using a single semiconductor optical amplifier," J. Lightwave Technol. **25**(1), 103–108 (2007).
28. M. Matsuura, O. Raz, F. Gomez-Agis, N. Calabretta, and H. J. S. Dorren, "320 Gbit/s wavelength conversion using four-wave mixing in quantum-dot semiconductor optical amplifiers," Opt. Lett. **36**(15), 2910–2912 (2011).
29. H. Hu, R. Nouroozi, R. Ludwig, B. Huettl, C. Schmidt-Langhorst, H. Suche, W. Sohler, and C. Schubert, "Polarization-insensitive all-optical wavelength conversion of 320 Gb/s RZ-DQPSK signals using a Ti:PPLN waveguide," Appl. Phys. B **101**(4), 875–882 (2010).
30. H. Hu, R. Nouroozi, R. Ludwig, B. Hüttl, C. Schmidt-Langhorst, H. Suche, W. Sohler, and C. Schubert, "Simultaneous polarization-insensitive wavelength conversion of 80-Gb/s RZ-DQPSK signal and 40-Gb/s RZ-OOK signal in a Ti:PPLN waveguide," J. Lightwave Technol. **29**(8), 1092–1097 (2011).
31. V. G. Ta'eed, M. R. E. Lamont, D. J. Moss, B. J. Eggleton, D.-Y. Choi, S. Madden, and B. Luther-Davies, "All optical wavelength conversion via cross phase modulation in chalcogenide glass rib waveguides," Opt. Express **14**(23), 11242–11247 (2006).
32. V. G. Ta'eed, L. Fu, M. Pelusi, M. Rochette, I. C. Littler, D. J. Moss, and B. J. Eggleton, "Error free all optical wavelength conversion in highly nonlinear As-Se chalcogenide glass fiber," Opt. Express **14**(22), 10371–10376 (2006).
33. J. Hansryd, P. A. Andrekson, M. Westlund, J. Li, and P.-O. Hedekvist, "Fiber-based optical parametric amplifiers and their applications," IEEE J. Sel. Top. Quantum Electron. **8**(3), 506–520 (2002).
34. R. W. Tkach, A. R. Chraplyvy, F. Forghieri, A. H. Gnauck, and R. M. Derosier, "Four-photon mixing and high-speed WDM systems," J. Lightwave Technol. **13**(5), 841–849 (1995).
35. Q. Lin, O. J. Painter, and G. P. Agrawal, "Nonlinear optical phenomena in silicon waveguides: modeling and applications," Opt. Express **15**(25), 16604–16644 (2007).
36. I. D. Rukhlenko, M. Premaratne, and G. P. Agrawal, "Nonlinear silicon photonics: analytical tools," IEEE J. Sel. Top. Quantum Electron. **16**(1), 200–215 (2010).
37. M. Pu, L. Liu, H. Ou, K. Yvind, and J. M. Hvam, "Ultra-low-loss inverted taper coupler for silicon-on-insulator ridge waveguide," Opt. Commun. **283**(19), 3678–3682 (2010).
38. M. Pu, H. Hu, M. Galili, H. Ji, C. Peucheret, L. Oxenlowe, K. Yvind, P. Jeppesen, and J. Hvam, "15-THz tunable wavelength conversion of picosecond pulses in a silicon waveguide," IEEE Photon. Technol. Lett. **23**(19), 1409–1411 (2011).

1. Introduction

Optical signal processing has been studied intensely over the last two decades, due to its potential for increased speed and in some contexts lower power consumption in future optical communication networks [1,2]. However, not all signal processing functionalities have a clear benefit from using all-optical schemes [3,4], and not all nonlinear optical materials are practical for making compact integrated multi-functional components. All-optical wavelength

#152339 - $15.00 USD Received 3 Aug 2011; revised 30 Aug 2011; accepted 30 Aug 2011; published 26 Sep 2011

conversion is one of the functionalities, which stands out as promising with a real potential for reduced energy consumption [3], especially for high serial line rates, where many bits may be processed in a single device. Silicon is a material that stands out due to its ultra-fast high nonlinearity, and its potential for monolithic integration enabling compact photonic circuitry [5]. This paper reports the fastest demonstrated all-optical signal processing in silicon to date, namely all-optical wavelength conversion of a 640-Gbit/s line-rate serial data signal.

Silicon is not only the second most abundant element in the Earth's crust, but its extensive use in electronics promises cheap mass production based on the abundant existing processing infrastructure. Silicon has attractive optical properties, such as a high refractive index, which makes it able to tightly confine light allowing for nano-scale optical devices and enhanced nonlinear optical effects, up to five orders of magnitude larger than that of silica glass fibers [6,7]. Four-wave mixing (FWM) in silicon has been used to demonstrate many all-optical functionalities, including parametric amplification, signal regeneration, waveform sampling, error-free demultiplexing and wavelength conversion [7–22]. However, silicon suffers from the slow dynamics of two-photon-absorption (TPA) induced free-carrier absorption (FCA), which usually limits the operation speed and introduces patterning effects [23]. This has limited most demonstrations to modest signal processing speeds, i.e. with control pulse rates in the few tens GHz range (10-80 GHz [7–21]). In wavelength conversion, the signal processing takes place at the aggregate bit rate, and here we experimentally demonstrate that it is indeed possible to operate at ultra-high bit rates such as 640 Gbit/s by low-power FWM in a 3.6-mm long silicon nanowire with a switching energy of ~110 fJ/bit. Bit error ratio measurements validate the performance within forward error correction (FEC) limits. The waveguide dispersion of the silicon nanowire is nano-engineered to optimize phase matching for FWM and the switching power used for the signal processing is low enough to reduce nonlinear absorption from TPA. This is the fastest photonic chip (595 Gbit/s net rate) demonstrated to date and this demonstration can potentially enable high-speed optical networks on a silicon photonic chip.

Wavelength conversion may play a key role in optical networks, by offering to resolve packet contention by transmitting at an alternate wavelength through the same route [24,25]. Compared to optical-electrical-optical (O/E/O) conversion schemes, all-optical wavelength conversion (AOWC) can offer advantages such as high speed (far beyond 100 Gbit/s) and potentially low power consumption. Great efforts have been made to achieve AOWC using different nonlinear media, including highly nonlinear fibers (HNLF) [25,26], semiconductor optical amplifiers (SOA) [27,28], periodically poled lithium niobate (PPLN) waveguides [29,30], chalcogenide waveguides or fibers [31,32], and silicon nanowires [14–22].

Silicon-based AOWC has attracted considerable research interest, due to its complementary metal-oxide-semiconductor (CMOS) compatibility, low cost, ultra-compactness, potential for integration with electronics, broad working bandwidth and high-speed operation [14–22]. However, silicon-based optical signal processing suffers from the slow dynamics of free carriers, which can introduce strong nonlinear absorption and resulting patterning effects. The carrier lifetime in silicon waveguides is typically of the order of several hundred picoseconds to several hundred nanoseconds [23], which usually limits the signal processing speed below 10 Gbit/s. Nevertheless, silicon-based optical signal processing has been demonstrated above 10 Gbit/s using different techniques to overcome these free-carrier induced speed limitations [11–13,19–22], including the use of a reverse-biased p-i-n diode structure for sweeping out the free carriers [20], a slot waveguide filled by a nonlinear material with simultaneous large Kerr coefficient and low absorption [13], or operation in the power regime where this nonlinear absorption is negligible [10,22]. Still, the control signal rate has mostly been modest, and only few attempts at increasing the rate into the hundreds Gbit/s range have been made [22]. In this work, we report the first demonstration of silicon-based all-optical wavelength conversion of data signals with up to 640 bit/s line-rate using FWM in a 3.6-mm long silicon nanowire, clearly showing the potential of ultra-high speed optical signal processing in silicon. The silicon nanowire is operated below significant TPA,

#152339 - $15.00 USD Received 3 Aug 2011; revised 30 Aug 2011; accepted 30 Aug 2011; published 26 Sep 2011

reducing the effect of photo-induced carriers, thereby favoring the ultra-fast Kerr-effect based FWM.

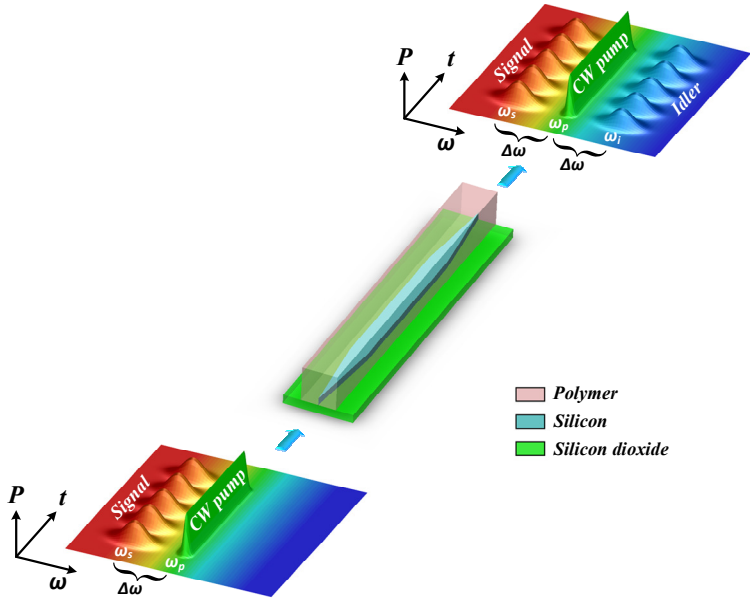

Fig. 1. Four-wave mixing in a silicon nanowire. A pump wave interacts with a signal wave and generates an idler wave at a new frequency of $2\omega_p - \omega_s$. The silicon nanowire is fabricated on a SiO_2/Si substrate, inversely tapered at each end and embedded into a larger polymer waveguide for low loss interfacing with optical fibers.

2. Four wave mixing (FWM) in a silicon nanowire

Wavelength conversion of a high-speed signal based on FWM in a silicon nanowire is illustrated in Fig. 1. In partially-degenerate FWM, a pump wave interacts with a signal wave in the silicon nanowire to generate an idler wave at a new frequency of $2\omega_p - \omega_s$. The generated idler wave replicates all the information (both amplitude and phase - though conjugated) of the signal, thus enabling wavelength conversion of a data signal. Effective FWM can be achieved if phase matching between the waves is ensured [33]. Considering both linear and nonlinear phase mismatch contributions, the phase mismatch κ is [33]

$$\kappa = \Delta\beta + 2\gamma P_{pump} \tag{1}$$

where $\Delta\beta = \beta_s + \beta_i - 2\beta_p$ is the linear phase mismatch due to dispersion, β_s, β_i and β_p are the propagation constants of the signal, idler and pump, respectively. The power dependent nonlinear phase mismatch is due to self-phase modulation (SPM) and cross phase modulation (XPM). P_{pump} is the pump power and γ is a nonlinear waveguide parameter. At moderate pump powers, the nonlinear phase mismatch can be neglected and the conversion efficiency (defined as the ratio of the idler power at the waveguide output to the signal power at the waveguide input) can be expressed in the undepleted-pump regime as [34]

$$G_{idler}(L) = \frac{P_{idler}(L)}{P_{signal}(0)} = \gamma^2 P_{pump}{}^2 L_{eff}^2 e^{-\alpha L} \eta \tag{2}$$

where

#152339 - $15.00 USD Received 3 Aug 2011; revised 30 Aug 2011; accepted 30 Aug 2011; published 26 Sep 2011

$$\eta = \frac{\alpha^2}{\alpha^2 + \Delta\beta^2}\left(1 + \frac{4e^{-\alpha L}\sin^2(\Delta\beta L/2)}{\left(1-e^{-\alpha L}\right)^2}\right) \tag{3}$$

and where $L_{eff} = \left(1-e^{-\alpha L}\right)/\alpha$ is the effective length of the waveguide and α is the waveguide loss per unit length. An efficient parametric conversion occurs when the linear phase mismatch $\Delta\beta$ is close to zero. At wavelengths around 1550 nm, bulk silicon has a very large normal GVD due to material dispersion (Fig. 2a). However, waveguide confinement can introduce anomalous GVD and overcome the material dispersion by nano-engineering the dimensions of the silicon waveguide, which will increase the conversion bandwidth. We simulated the coupled effects of material and waveguide dispersion using a custom-made finite-difference mode solver to calculate the total GVD for the propagating mode. Figure 2a shows the simulated GVD for the transverse-electric (TE) mode of silicon waveguides with different dimensions. At moderate pump powers the impact of free carriers is negligible [35] and only the Kerr nonlinearity needs to be considered. Based on the calculated dispersion curves, the FWM efficiency can be computed using Eq. (2). Figure 2b shows the simulated conversion bandwidth for silicon waveguides with different dimensions. It was ensured, using full numerical simulations by the split-step Fourier method, that Eq. (2) could accurately predict the conversion efficiency at the employed pump power level. The 450 × 240 nm^2 waveguide has a zero-dispersion wavelength of ~1550 nm and a small GVD within the telecommunication C band (1530 nm – 1560 nm), allowing for ultra-broadband phase matching and an ultra-broad conversion bandwidth of 330 nm. The 450 × 200 nm^2 waveguide and the 450 × 300 nm^2 waveguide exhibit relatively large GVDs, thus resulting in a narrower conversion bandwidth than the 450 × 240 nm^2 waveguide. As the conversion bandwidth is of importance for wavelength conversion of an ultra-high speed data signal having a broad spectrum, the waveguide with cross section dimension 450 × 240 nm^2 was used to perform the wavelength conversion experiment. The inset of Fig. 2b shows the measured conversion efficiency for the silicon nanowire with the cross section dimension of 450 × 240 nm^2. The conversion efficiency is almost constant within the range from 1520 nm to 1620 nm, which is only limited here by the tuning range of the available laser.

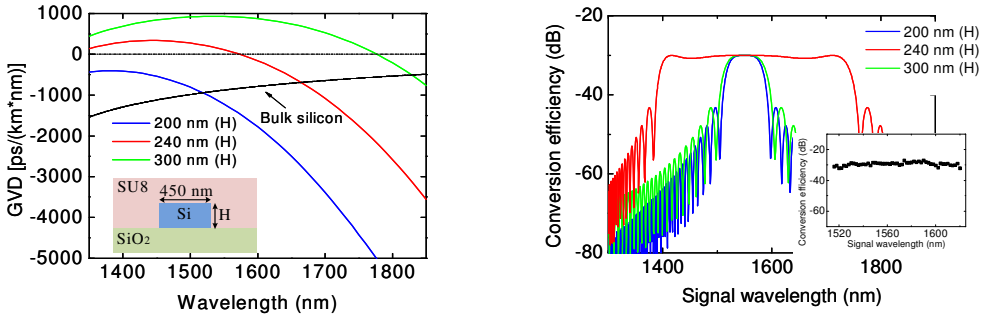

(a) (b)

Fig. 2. (a) Simulated GVD and (b) FWM conversion efficiency of the silicon waveguide with 450-nm width and different heights (200 nm, 240 nm, 300 nm). Inset. Measured conversion efficiency at the pump wavelength of 1550 nm for the waveguide with cross section 450 × 240 nm^2.

3. Two photon absorption (TPA) and free carrier absorption (FCA)

During the FWM process, the parasitic TPA-induced FCA could result in additional nonlinear absorption and patterning effects, which could limit the conversion efficiency and operation speed. We investigated the FCA by measuring the insertion losses of the device for different coupled peak powers. Figure 3a shows that the insertion loss increases slowly when the

#152339 - $15.00 USD Received 3 Aug 2011; revised 30 Aug 2011; accepted 30 Aug 2011; published 26 Sep 2011

coupled peak power is relatively low but increases dramatically when the coupled peak power exceeds a TPA threshold of ~39 dBm. This power threshold is also verified to exist by observing the spectral shifting, which is associated with the free carriers [36]. The FCA and the free-carrier dispersion (FCD) effects can shift the output spectrum towards shorter wavelengths (so called free-carrier induced blue shift). As shown in Fig. 3b, the output optical spectrum has no blue shift when the input power is below the threshold, while a strong blue shift and even an asymmetric blue spectral broadening are observed when the coupled power is well above the threshold (peak power of 45 dBm). Thus, working at the power regime below the threshold can strongly reduce the effect of TPA and FCA.

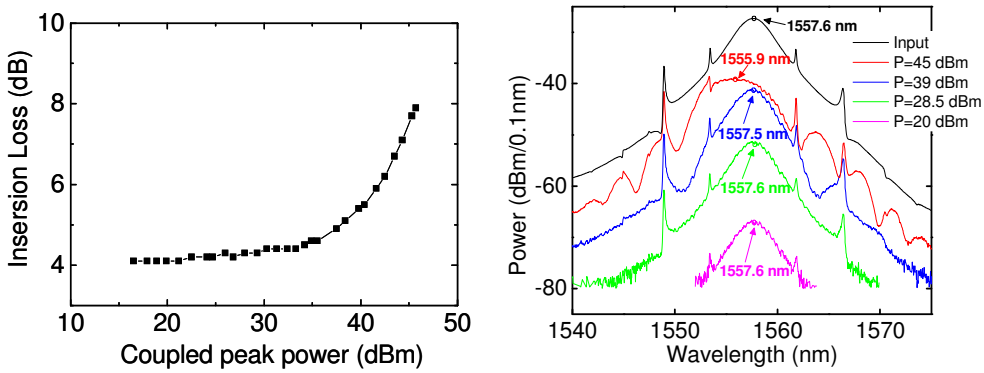

(a) (b)

Fig. 3. (a) Free-carrier induced nonlinear absorption for the 3.6-mm long silicon waveguide with cross section 450 × 240 nm^2. The insertion loss is measured for different coupled peak powers. It is clearly shown that when the peak power is below the TPA threshold (~39 dBm) the nonlinear absorption is almost negligible (<1 dB nonlinear loss) and when the peak power is above the threshold the nonlinear absorption increases significantly. (b) Optical spectra at the output of the silicon waveguide for different input powers. For a power above the threshold, the free-carrier induced spectral blue-shift and a broadening of the spectrum is observed.

4. Wavelength conversion experiment

The key device in the wavelength converter is the dispersion engineered straight 3.6-mm long silicon waveguide, which includes tapering sections for low-loss interfacing with optical fiber. The main waveguide section is ~3 mm long and has a cross section of 450 × 240 nm^2 while the tapering sections are ~0.3 mm long each and their width is inversely tapered from 450 nm to 20 nm [37]. This tapering enables coupling between the silicon waveguide and the larger polymer waveguide (SU8-2005) into which the whole silicon structure is embedded. The cross section (3.4 × 3.4 μm^2) of the polymer waveguide matches the tapered access fibers, reducing the fiber coupling loss to 1.5 dB per facet. The device has a silicon-on-insulator (SOI) structure, with the silicon waveguide placed on a SiO_2/Si substrate. The measured propagation loss is 4.3 dB/cm and the fiber-to-fiber loss of the device is 4.5 dB.

The experimental setup for silicon-based wavelength conversion of a 640-Gbit/s return-to-zero differential phase-shift keying (RZ-DPSK) signal is shown in Fig. 4d. In the 640-Gbit/s transmitter, the 10-GHz pulse train is generated from a mode-locked laser and then compressed to 600 fs in a 400-m dispersion-flattened highly nonlinear fiber [25]. The compressed pulses are DPSK modulated by a 10-Gbit/s pseudo-random binary sequence (PRBS) of length $2^{31} - 1$ in a Mach-Zehnder modulator (MZM). The modulated 10-Gbit/s DPSK signal is multiplexed in time to 640 Gbit/s using a passive fiber-delay multiplexer (MUX × 64). The generated 640-Gbit/s RZ-DPSK signal at 1562 nm is launched into the silicon waveguide with an averaged coupled power of 16 dBm together with a continuous wave (CW) pump at 1550 nm through a 3-dB optical coupler. The coupled pump power is 18.5 dBm, which corresponds to a switching energy of only ~110 fJ/bit. The optical spectra at

#152339 - $15.00 USD Received 3 Aug 2011; revised 30 Aug 2011; accepted 30 Aug 2011; published 26 Sep 2011

the input and the output of the silicon waveguide are shown in Figs. 4a and b. After filtering and amplification, the wavelength converted 640-Gbit/s RZ-DPSK signal at 1538 nm is extracted from the pump and signal (Fig. 4c). The spurious peaks in the spectrum are due to XPM induced by the data signal on the CW pump. The wavelength converted signal is also characterized in the time domain by measuring autocorrelation traces (Fig. 4g). Compared to the input data pulse (FWHM of 600 fs, Fig. 4e) the wavelength converted data pulse is slightly broadened to a FWHM of 640 fs, which is mainly an effect of the filtering subsystem.

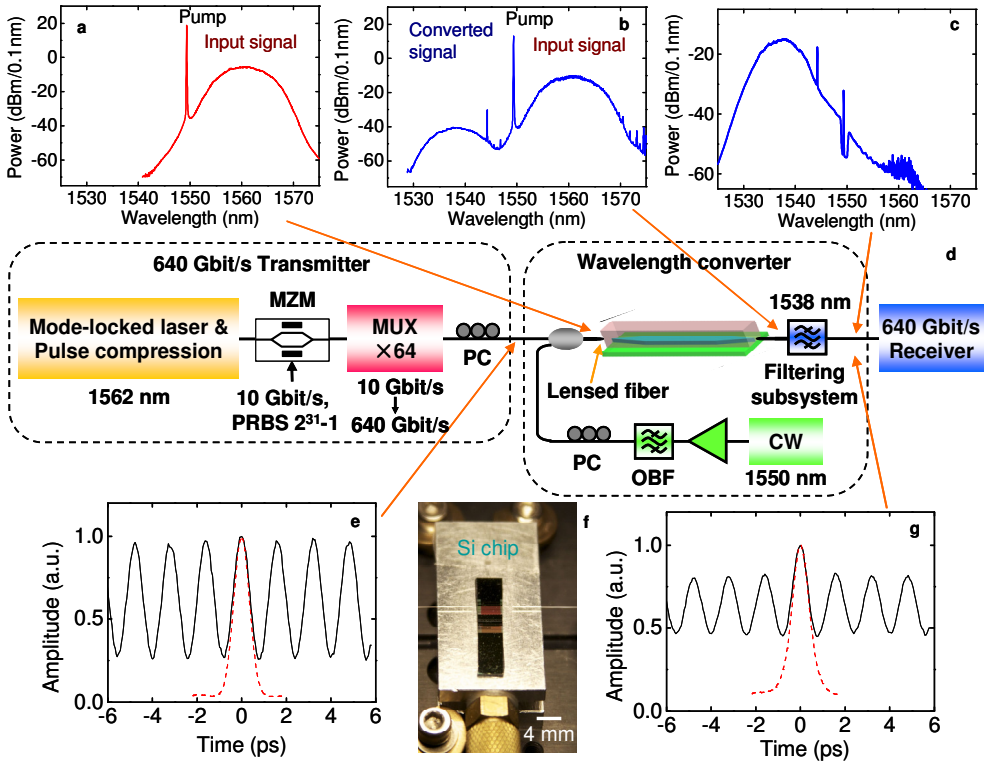

Fig. 4. Experimental setup for all-optical wavelength conversion on a silicon photonic chip. A 640-Gbit/s transmitter consists of a short pulse source (600 fs of FWHM), a Mach Zehnder data modulator (MZM) and an optical time-division multiplexer (MUX). The wavelength converter consists of a silicon chip, a CW laser, an erbium-doped fiber amplifier, an optical bandpass filter (OBF), a polarization controller (PC) and a filtering subsystem. (a) Spectrum at the input of the silicon chip. (b) Spectrum at the output of the silicon chip. (c) Spectrum of the converted signal after filtering and amplification. (e) Autocorrelation trace of the input signal. (f) Photograph of the silicon photonic chip. (g) Autocorrelation trace of the converted signal.

The converted 640-Gbit/s OTDM signal is detected in a 640-Gbit/s OTDM receiver, which consists of a nonlinear optical loop mirror (NOLM) based OTDM demultiplexer, an 0.9-nm filter and a 10-Gbit/s DPSK receiver. The NOLM is used to demultiplex the 640-Gbit/s serial data signal to a 10-Gbit/s data signal based on cross-phase modulation (XPM) in a 50-m HNLF. Then, the demultiplexed 10-Gbit/s RZ-DPSK signal is demodulated by a delay-line interferometer and detected by a balanced photodetector. The quality of the wavelength converted signal is quantified by performing bit error ratio (BER) measurements (Fig. 5). The wavelength-converted 640-Gbit/s RZ-DPSK signal achieves a BER well below the standard forward-error correction (FEC, 7% overhead) limit of 2×10^{-3} for all 64 tributaries, but with a significant error floor at ~10^{-4}, which is expected to be due to the reduced OSNR, stemming from the relatively low conversion efficiency, and the slight pulse broadening. This result corresponds to a post-FEC error-free performance (BER < 10^{-12}) at a

#152339 - $15.00 USD Received 3 Aug 2011; revised 30 Aug 2011; accepted 30 Aug 2011; published 26 Sep 2011

net data rate of 595 Gbit/s. For lower bit rates such as 160 Gbit/s and 320 Gbit/s, the wavelength converted signals achieved a BER of 10^{-9}, signifying good performance of the photonic chip. The insets of Fig. 5 show the demultiplexed eye diagrams from the wavelength converted RZ-DPSK signals.

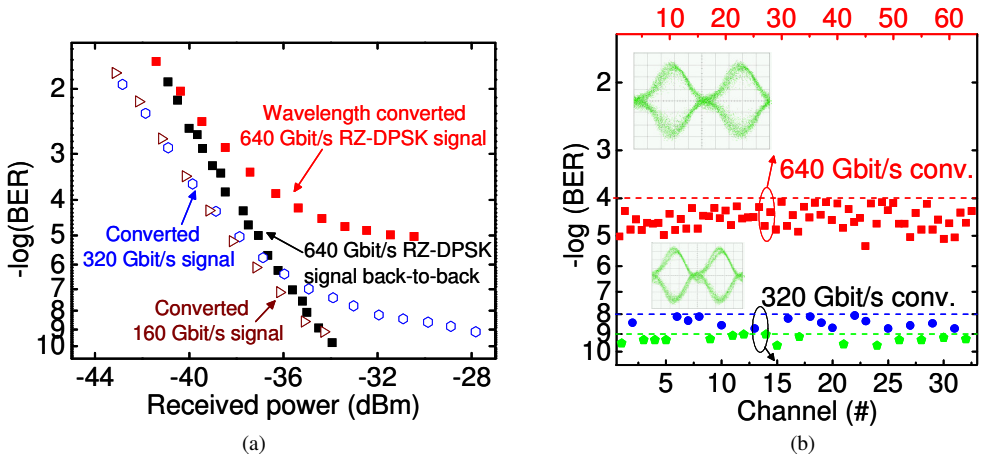

(a) (b)

Fig. 5. BER measurements for the wavelength-converted signal and corresponding eye diagrams. (a) BER curves for the wavelength converted 160 Gbit/s, 320 Gbit/s, 640 Gbit/s DPSK data signals and the back-to-back 640 Gbit/s signal. (b) BER for all the OTDM tributaries of the converted 640 Gbit/s and 320 Gbit/s signals. Inset: corresponding eye diagrams.

The error floor of the BER measurements could be lowered with higher conversion efficiency if the power level is raised or the propagation loss is reduced. The total launched power in this experiment is only 20.4 dBm, which is well below the TPA threshold; therefore the conversion efficiency is not limited by the intrinsic nonlinear absorption. In another experiment using a pulsed pump with a peak power of 34.7 dBm, the conversion efficiency is increased to −16.5 dB [38]. In addition, the high average launched power could result in facet damage of the polymer waveguide, but it can be avoided by increasing the cross-sectional area. If the cross section of the polymer is increased to 9×9 μm^2, which fits the diameter of the standard single mode fiber core, the sustainable launched power would be greatly

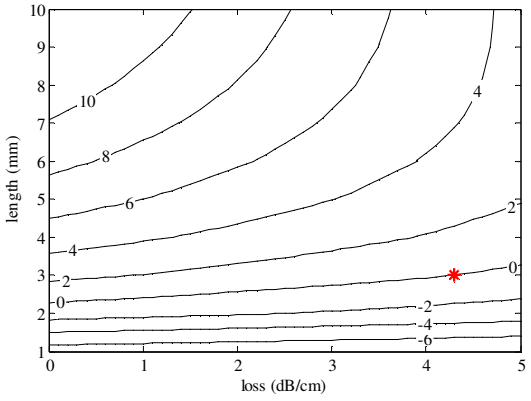

Fig. 6. Conversion efficiency gain (in dB) as a function of propagation loss and waveguide length relatively to the reference case of a 3-mm long waveguide with 4.3 dB/cm loss (indicated by a red star).

#152339 - $15.00 USD Received 3 Aug 2011; revised 30 Aug 2011; accepted 30 Aug 2011; published 26 Sep 2011

increased. On the other hand, the propagation loss (4.3 dB/cm) of our silicon nanowire is relatively high compared to state of the art (~1 dB/cm) [16], which limits the effective length of the waveguide. Therefore, a longer silicon nanowire with a lower propagation loss would also increase the conversion efficiency. Figure 6 shows the possible improvement of the conversion efficiency for lower propagation loss and longer waveguide compared to the silicon nanowire used in the experiment (propagation loss of 4.3 dB/cm and length of 3 mm) assuming the same pump power is used in all cases.

5. Conclusion

We have successfully demonstrated all-optical wavelength conversion of a 640-Gbit/s line-rate (595 Gbit/s net rate) RZ-DPSK signal based on low-power FWM in a silicon photonic chip with a switching energy of only ~110 fJ/bit. These results demonstrate that high-speed wavelength conversion is achievable in silicon chips with high data integrity and indicate that high-speed operation can be obtained at moderate power levels where nonlinear absorption due to TPA and FCA is not detrimental. These results constitute the highest serial signal processing speed in silicon or any chip demonstrated to date. We believe this is an important confirmation of the great potential of silicon for high-speed optical signal processing.

Acknowledgments

We would like to acknowledge the Danish Research Council for supporting the NOSFERATU project and the European Research Council for supporting the SOCRATES project.

#152339 - $15.00 USD Received 3 Aug 2011; revised 30 Aug 2011; accepted 30 Aug 2011; published 26 Sep 2011